

# Measurement of large aspheric surfaces by annular subaperture stitching interferometry

Xiaokun Wang (王孝坤)<sup>1,2</sup>, Lihui Wang (王丽辉)<sup>1,2</sup>, Longhai Yin (殷龙海)<sup>1</sup>,  
Binzhi Zhang (张斌智)<sup>1</sup>, Di Fan (范 镛)<sup>1</sup>, and Xuejun Zhang (张学军)<sup>1</sup>

<sup>1</sup>Changchun Institute of Optics, Fine Mechanics and Physics, Chinese Academy of Sciences, Changchun 130033

<sup>2</sup>Graduate School of the Chinese Academy of Sciences, Beijing 100039

Received May 16, 2007

A new method for testing aspheric surfaces by annular subaperture stitching interferometry is introduced. It can test large-aperture and large-relative-aperture aspheric surfaces at high resolution, low cost, and high efficiency without auxiliary null optics. The basic principle of the method is described, the synthetical optimization stitching model and effective algorithm are established based on simultaneous least-square fitting. A hyperboloid with an aperture of 350 mm is tested by this method. The obtained peak-to-valley (PV) and root-mean-square (RMS) values of the surface error after stitching are  $0.433\lambda$  and  $0.052\lambda$  ( $\lambda$  is 632.8 nm), respectively. The reconstructed surface map is coincide with the entire surface map from null test, and the difference of PV and RMS errors between them are  $0.031\lambda$  and  $0.005\lambda$ , respectively. This stitching model provides another quantitative method for testing large aspheric surfaces besides null compensation.

OCIS codes: 220.4840, 120.3940, 120.3180, 070.4560.

Aspheric surfaces can correct aberrations, improve the image quality, and reduce the size and weight of optical systems. So they are extremely important in optical systems and have been applied in various fields<sup>[1,2]</sup>. Since the curvature of asphere is variable in different regions, the fabrication and measurement are more difficult than spherical and flat surfaces. Especially when testing large aperture, steep, and large departure aspheric surfaces, many interference fringes are formed on the detection device and make proper analysis difficult to perform, so we will fall back on auxiliary optics such as null corrector and computer-generated holograms (CGHs)<sup>[3]</sup>. The auxiliary element must have been specially designed and customized, and it brings manufacturing errors and some unavoidable misalignment errors. The cost of making and verifying the null elements conspires to keep aspheres from practical optical designs.

Annular subaperture stitching (ASS) can expand the dynamic range of interferometer, and broaden the measurement scope significantly. It can test large-aperture, high-numerical-aperture aspheric surfaces at high resolution, low cost, and high efficiency without any null optics. There are two mathematic models for this method at present. Liu *et al.* calculated the full-aperture Zernike coefficients from the subaperture Zernike coefficients obtained by commercial interferogram reduction software<sup>[4]</sup>. Since Zernike circle polynomials are not orthogonal over annular region, the fitting results may give wrong results. Recently Hou *et al.* modified the stitching algorithm with Zernike annular polynomials instead of Zernike circle polynomials<sup>[5,6]</sup>. They calculated the Zernike annular polynomials for each subaperture, and then fitted the Zernike polynomial coefficients for the entire. The results of numerical simulations showed that the modified algorithm has a better performance. Another stitching model with successive overlapping phase maps was presented by Melozzi *et al.*<sup>[7]</sup>. They stitched two adjacent phase maps by elim-

inating the misalignment errors through fitting phase data with Zernike annular polynomials over the common zones. This process was then repeated until the whole aperture was covered, thus the full phase distribution could be derived.

Since the two algorithms carry on the Zernike annular polynomials fitting, they are very complicated and the mid- and high-frequency errors might be "smoothed out" after stitching. The second model sews annular subapertures one by one, the splicing errors will accumulate. Although the theory and algorithm have been researched for many years, testing large aspheric surfaces by ASS have almost not been reported experimentally.

In this letter, we introduce a novel optimizing stitching model for testing aspheric surfaces by ASS. The data processing is simple and it can prevent the error from accumulation. We have measured a large asphere by ASS and applied it to the practical engineering.

The principle and process of ASS are very crucial. Figure 1 shows the sketch of the experimental setup. At first, we choose the proper transmission sphere and decide the number of subapertures. Then we align the interferometer and the tested asphere, make the center of curvature of the spherical wavefront coincide with the asphere. The slope of the spherical wavefront matches

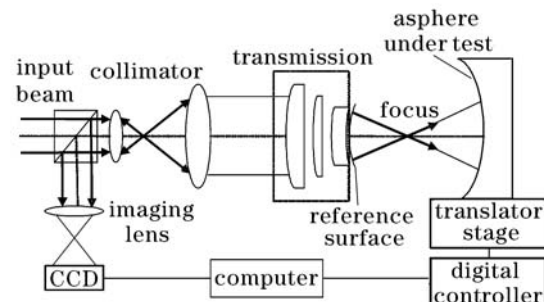


Fig. 1. Schematic of the setup with annular subaperture stitching.

that of the central area, so the fringes in the central portion of the interferogram are well distinguished, recording the phase distribution of this region. But the fringes in the outer portion are denser, the fringe density often exceeds 2 pixels/wave. The fringe pattern is aliased in that area and it exceeds the resolution of the charge-coupled device (CCD). By varying the distance from the asphere to the interferometer, the slope of the spherical wavefront becomes smaller and matches that of the aspheric surface in the outer annular zone, so the null zone moves from the central region to an outer region<sup>[7,8]</sup>. This process is then repeated to make spherical reference wavefronts with different curvature radii match the corresponding annular subapertures and let the adjacent subapertures have some superposition. When the entire aperture is covered, the corresponding phase data of each annular subaperture can be obtained by interferometry. Then the relative translation error is subtracted from each subaperture through the simultaneous least-square method. Finally, after all the translation errors have been removed, a least-square fitting with the full data is performed to evaluate the misalignment errors of the system.

We can stitch two annular subapertures by subtracting the translation errors of adjacent subapertures<sup>[9]</sup>. Using the principle of two-subaperture splicing from many times may realize multi-subaperture stitching. But it often brings the erroneous transmission and accumulation, thus reduces the precision. In this letter, the sum of the squared differences for all common areas should be minimized simultaneously<sup>[10]</sup>.

Suppose there are  $M$  subapertures altogether. In order to simplify the localization and test, generally choosing the subaperture in the center region of the aspheric surface for the reference standard, each measurement needs to hold the following function for the correction of piston, tilt, and power:

$$\begin{aligned} w_0 &= w_1 + a_1x + b_1y + c_1(x^2 + y^2) + d_1 \\ &= w_2 + a_2x + b_2y + c_2(x^2 + y^2) + d_2 = \dots \\ &= w_{M-1} + a_{M-1}x + b_{M-1}y + c_{M-1}(x^2 + y^2) + d_{M-1}, \end{aligned} \quad (1)$$

$$\begin{bmatrix} A \\ B \\ C \\ D \end{bmatrix} = \begin{bmatrix} \sum xx & \sum xy & \sum x(x^2 + y^2) & \sum x \\ \sum yx & \sum yy & \sum y(x^2 + y^2) & \sum y \\ \sum (x^2 + y^2)x & \sum (x^2 + y^2)y & \sum (x^2 + y^2)^2 & \sum (x^2 + y^2) \\ \sum x & \sum y & \sum (x^2 + y^2) & n \end{bmatrix}^{-1} \begin{bmatrix} \sum x\Phi \\ \sum y\Phi \\ \sum (x^2 + y^2)\Phi \\ \sum \Phi \end{bmatrix}. \quad (5)$$

After calculating these coefficients, we can obtain the exact figure error of the asphere by removing these polynomials.

We have tested an asphere (diameter  $D = 350$  mm, radius of curvature at the vertex  $R_0 = 4188.04$  mm, conic constant  $k = -2.816915$ ) by ASS using the experimental setup shown in Fig. 2. The results of three individual measurements are given in Figs. 3 and 4 (the fiducial circular subaperture and two outer annular subapertures,  $r$  is the normalized radius of the full aperture,  $0 \leq r \leq 1$ ). Then the translation error was eliminated from each sub-

aperture,  $w_0$  is the phase distribution of the fiducial subaperture,  $w_1, w_2, \dots, w_{M-1}$  are the phase distributions of other annular subapertures, and  $a_i, b_i, c_i, d_i$  are the coefficients of the relative translation errors to the fiducial subaperture of the tilt in the  $x$  and  $y$  directions, power, and displacement, respectively. By using least-square fitting, we should minimize the sum of the squared differences in the all overlapping regions as

$$\begin{aligned} S &= \sum_{i=1}^n [w_1 + a_1x + b_1y + c_1(x^2 + y^2) + d_1 - w_0]^2 \\ &+ \sum_{j=1}^{M-2} \sum_{i=1}^n \{ [w_{j+1} + a_{j+1}x + b_{j+1}y \\ &+ c_{j+1}(x^2 + y^2) + d_{j+1}] \\ &- [w_j + a_jx + b_jy + c_j(x^2 + y^2) + d_j] \}^2 = \min, \end{aligned} \quad (2)$$

where  $n$  is the number of sampling points of each common region, the total number of all overlapping regions is  $M - 1$ . Taking the differentiations of Eq. (2) with respect to these unknowns, the least squares equation can be described as

$$\frac{\partial S}{\partial a_j} = 0, \quad \frac{\partial S}{\partial b_j} = 0, \quad \frac{\partial S}{\partial c_j} = 0, \quad \frac{\partial S}{\partial d_j} = 0, \quad (3)$$

where  $j$  is an integer from 1 to  $M - 1$ . The best stitching parameters can be obtained by Eq. (3).

When all the translation errors have been eliminated, a least-square fitting is performed to evaluate the misalignment errors of the whole system:

$$\sum_{i=1}^N \{ w(x_i, y_i) - [Ax_i + By_i + C(x_i^2 + y_i^2) + D] \}^2 = \min, \quad (4)$$

where  $w$  is the phase distribution of the full aperture,  $N$  is the number of the total sampling points,  $A, B, C, D$  are the misalignment coefficients of the system, which can be derived from

aperture by the simultaneous least-square method. At last, a final least-square fitting was performed to derive the misalignment errors of the system. The surface map of the full aperture synthesized by the stitching method is given in Fig. 5, where the peak-to-valley (PV) error is  $0.433\lambda$  and root-mean-square (RMS) error is  $0.052\lambda$ .

For comparison, the asphere was also tested by null compensation. Figure 6 gives the surface map and interferogram from the null test, where the PV and RMS errors are  $0.402\lambda$  and  $0.047\lambda$ , respectively. The differences of PV and RMS errors between the two methods

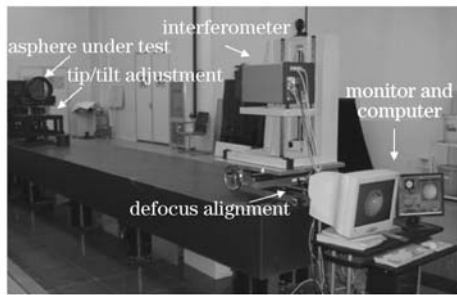


Fig. 2. Experimental setup.

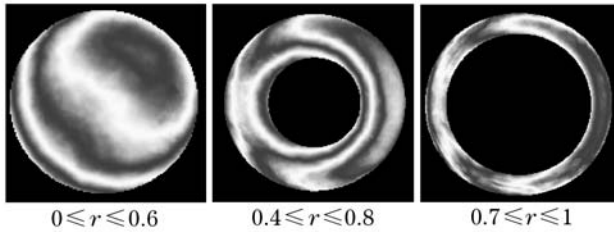


Fig. 3. Interferograms of three subapertures obtained with annular mask.

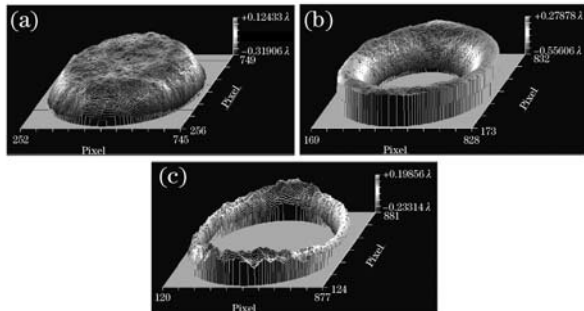
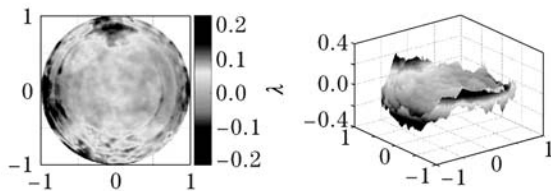


Fig. 4. Corresponding phase distributions of three subapertures.

Fig. 5. Normalized surface map of the whole aperture by stitching method. PV:  $0.433\lambda$ , RMS:  $0.052\lambda$ .

are  $0.031\lambda$  and  $0.005\lambda$ , respectively. And the surface maps from the two methods are consistent. Although only three subapertures are used to cover the full aperture in this experiment, the same stitching procedure can be extended to test larger and steeper aspheric surfaces with more annular subapertures.

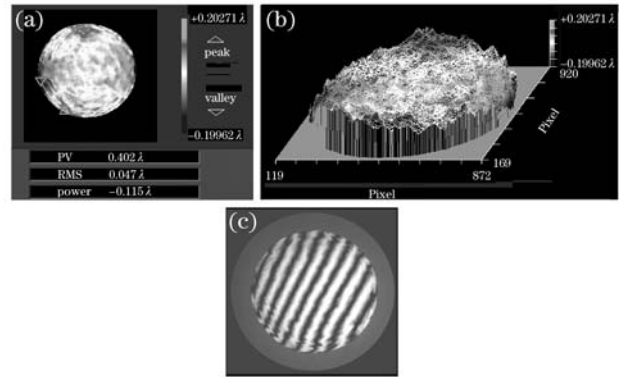


Fig. 6. Surface map and interferogram by null compensation.

In conclusion, we have proposed a synthetic optimization stitching model for testing large asphere. The stitching algorithm is based on a simultaneous least-square minimization of the mismatch among all overlapping regions, and the data processing is simple and clear. It avoids error transmission and Zernike annular polynomial fitting, and the mid- and high-frequency errors are not “smoothed out” after stitching. The measurement results for a large-aperture asphere conclude that this mathematical model and stitching algorithm are feasible and effective.

X. Zhang is the author to whom the correspondence should be addressed, his e-mail address is zhangxj@ciomp.ac.cn.

## References

1. H. Kurita, K. Saito, M. Kato, and T. Yatagai, Proc. SPIE **680**, 47 (1986).
2. J. Ruckman, E. Fess, and D. Van Gee, Proc. SPIE **3782**, 2 (1999).
3. J. Chang, F. Li, Z. Weng, Z. Zhang, H. Jiang, and X. Cong, Acta Opt. Sin. (in Chinese) **23**, 1266 (2003).
4. Y.-M. Liu, G. N. Lawrence, and C. L. Koliopoulos, Appl. Opt. **27**, 4504 (1988).
5. X. Hou, F. Wu, L. Yang, S. Wu, and Q. Chen, Chin. Opt. Lett. **4**, 211 (2006).
6. X. Hou, F. Wu, L. Yang, S. Wu, and Q. Chen, Appl. Opt. **45**, 3442 (2006).
7. M. Melozzi, L. Pezzati, and A. Mazzoni, Opt. Eng. **32**, 1073 (1993).
8. X. Wang and X. Zhang, Opt. Technique (in Chinese) **32**, 673 (2006).
9. F. Granados-Agustín, F. Escobar-Romero, and A. C. Rodríguez, Proc. SPIE **4829**, 44 (2003).
10. X. Wang, X. Zhang, L. Wang, and L. Zheng, Opt. Precision Eng. (in Chinese) **14**, 527 (2006).